ELSEVIER

Catalysis Today 40 (1998) 263–272

CATALYSIS TODAY

Vanadium phosphorus oxides with P/V=2 used as oxidation and ammoxidation catalysts

F.K. Hannour[1,a], A. Martin[a,*], B. Kubias[a], B. Lücke[a], E. Bordes[b], P. Courtine[b]

[a] *Institut für Angewandte Chemie Berlin-Adlershof e.V., Rudower Chaussee 5, D-12489 Berlin, Germany*
[b] *Département de Génie Chimique, Université de Technologie de Compiègne, BP 649, F-60206 Compiègne Cedex, France*

Abstract

Vanadium polyphosphates with a molar ratio of P/V=2 (α-$VO(PO_3)_2$, β-$VO(PO_3)_2$ and amorphous as well as partly crystalline $VO(PO_3)_2$) and $NH_4VP_2O_7$ were synthesized, characterized by chemical and thermal analysis, X-ray diffraction and FTIR spectroscopy and used as catalysts in the oxidation of *n*-butane to maleic anhydride (MA) as well as in the ammoxidation of toluene to benzonitrile. The results are compared with the catalytic properties of $V(PO_3)_3$ (P/V=3), $(NH_4)_2(VO)_3(P_2O_7)_2$ (P/V=4/3) and $(VO)_2P_2O_7$ (P/V=1). The MA selectivities of the amorphous $VO(PO_3)_2$ and of the crystalline α- and β-$VO(PO_3)_2$ are comparable to one another, whereas the specific rate per area of MA formation of the amorphous as well as partly crystalline $VO(PO_3)_2$ strongly differs from the rates of the crystalline solids. The amorphous catalyst reveals a rate similar to that of the $(VO)_2P_2O_7$ catalyst, but a lower MA selectivity. Contrary to other studies, only traces of furan were found and the total oxidation products CO and CO_2 were detected on all catalysts at very low conversion. Surprisingly, $V(PO_3)_3$ exhibits remarkable activity and MA selectivity. The crystalline polyphosphates show a lower activity in the ammoxidation of toluene compared with the amorphous $VO(PO_3)_2$ as well as $NH_4VP_2O_7$ and the benzonitrile selectivity reaches a value of ≈85%. Noticeable benzaldehyde amounts could be detected, especially at low conversion rates, proving its role as a reaction intermediate. © 1998 Elsevier Science B.V.

Keywords: Vanadium phosphate catalysts; Catalyst formation; Oxidation; Ammoxidation

1. Introduction

Vanadium phosphorus oxides (VPO) are well known as catalysts of the partial oxidation of *n*-butane to maleic anhydride (MA) (e.g. Refs. [1–3]) and of the ammoxidation of methylaromatics and methylheterocycles to the corresponding nitriles (e.g. [4,5]). Oxovanadium(IV)-diphosphate $(VO)_2P_2O_7$ (P/V=1) is considered to be the active and selective crystalline phases of *n*-butane oxidation VPO catalysts [1–3]. This phase is mostly generated from the precursor phase $VOHPO_4{\cdot}1/2H_2O$ via a topotactic transformation during the catalyst activation (e.g. [1,2]). $VOHPO_4{\cdot}1/2H_2O$ can also be used as a precursor phase of ammoxidation catalysts [4,6]; however, a more drastic structural transformation, mainly into $(NH_4)_2(VO)_3(P_2O_7)_2$ proceeds during pretreatment in the presence of the ammoxidation feed [7,8].

Several investigations of the surface properties of $(VO)_2P_2O_7$-based *n*-butane oxidation catalysts

*Corresponding author.

[1]On leave from the Department of Chemical Engineering, University of Technology of Compiègne, France.

0920-5861/98/$32.00 © 1998 Elsevier Science B.V. All rights reserved.
PII S0920-5861(98)00014-5

revealed an enrichment in phosphorus in the catalyst surface (e.g. [9,10]). It is assumed that, besides other reasons, this enrichment is responsible for a high maleic anhydride (MA) selectivity [11–13]. However, a too high P/V ratio in the parent solution, used during the synthesis of the $VOHPO_4 \cdot 1/2H_2O$ precursor, leads to catalysts with minor activity [9,14]. $VO(H_2PO_4)_2$ is formed under these conditions besides the desired $VOHPO_4 \cdot 1/2H_2O$ [14] and $VO(PO_3)_2$ is obtained by calcination of this compound [15]. The occurrence of $VO(PO_3)_2$ besides $(VO)_2P_2O_7$ causes low-surface-area catalysts and this is thought to be responsible for a decrease in activity [14]. Therefore, its presence in $(VO)_2P_2O_7$ catalysts should be avoided [16]. On the other hand, the specific rate per area of MA formation on $VO(PO_3)_2$ was found to be comparable to that of $(VO)_2P_2O_7$ [14].

In a previous study on the catalytic properties of $VO(PO_3)_2$-containing catalysts, a minor MA selectivity was reported [17]. In contrast, an MA selectivity of more than 40% was found recently on β-$VO(PO_3)_2$ which was nearly independent on the degree of the *n*-butane conversion, being between 5 and 70% [18]. More recently, on an amorphous $VO(PO_3)_2$ catalyst a very different selectivity behaviour has been reported at low *n*-butane conversion (<10%) [19,20]. According to the authors, only the products of partial oxidation are formed under these conditions. Besides the formation of MA, a selectivity of furan up to 40% has been claimed at an *n*-butane conversion of 2%. The specific rate per area of MA formation proved to be comparable to or higher than that measured on a P/V=1 catalyst, in accordance with the finding described in [14]. It was concluded that a new route of MA synthesis without the formation of carbon oxides could be achieved, using catalysts with a phosphorus-rich surface. Therefore, according to the authors, the application of catalysts with P/V=2 would be important if such a catalyst with higher surface area could be prepared [20].

To our knowledge, the catalytic properties of VPO catalysts with P/V=2 during the ammoxidation of methylaromatics have never been investigated so far. Only a P/V=2 derivative, the diammonium oxovanadium(IV)-diphosphate $(NH_4)_2VOP_2O_7$, was used as catalyst in the ammoxidation of methylaromatics [4,21]. A phase transformation was observed after contact with the ammoxidation feed, generating crystalline $NH_4VP_2O_7$ as identified by X-ray diffractometry (XRD), and has been described in detail in Ref. [21].

Against this background, it was the aim of the present work to investigate the activity and selectivity of the crystalline polyphosphates α- and β-$VO(PO_3)_2$ and of amorphous $VO(PO_3)_2$ in the oxidation of *n*-butane to MA. Furthermore, the different oxovanadium polyphosphates and $NH_4VP_2O_7$ (generated from the $VO(H_2PO_4)_2$ precursor by heating in the presence of ammoxidation feed) were used as catalysts in the ammoxidation of toluene to benzonitrile. Additionally, the catalytic properties of $(VO)_2P_2O_7$, $V(PO_3)_3$ and of a catalyst obtained from $VOHPO_4 \cdot 1/2H_2O$ precursor under ammoxidation conditions ($(NH_4)_2(VO)_3(P_2O_7)_2+V_xO_y$) were also studied in order to derive relationships between structure and catalytic performance.

2. Experimental

2.1. Precursor compounds and catalysts

The precursor $VO(H_2PO_4)_2$ (VHP/2) was synthesized by mixing and heating V_2O_5 (1 mol), H_3PO_4 (6 mol) and water (400 ml) in the presence of an excess of oxalic acid (1.2 mol) at 363 K for 48 h [22]. The resulting blue, V^{4+} ion-containing solution was evaporated overnight. The obtained solid was powdered, washed with acetone and dried. Characterization by chemical analysis and XRD confirmed the material to be VHP/2. The material was then calcined (heating rate=10 K/min) in the presence of air and, depending on the final temperature applied, the tetragonal β-$VO(PO_3)_2$ (β-VP/2, 1073 K, 1 h) or the amorphous product VP/2-1 (673 K, 6 h) and the partly crystalline VP/2–2 (773 K, 24 h; 60–75% β-$VO(PO_3)_2$ besides other polyphosphates) were obtained. The monoclinic α-$VO(PO_3)_2$ (α-VP/2) was directly synthesized by heating V_2O_5 (0.055 mol) in an excess of H_3PO_4 (1.72 mol) at 643 K for 5 h under air (heating rate=10 K/min), according to the method described in Ref. [23]. A mixture of both modifications (α/β-VP/2) was obtained in the same way at a reaction temperature of 693 K.

$NH_4VP_2O_7$ (NVP/2) was generated by transformation of VHP/2 (0.023 mol) at 673 K for 5 h (heating

Table 1
Chemical analysis data, vanadium valence state and BET surface areas of the parent samples

Sample	P/V molar ratio	H/N molar ratio	V valence state	BET ($m^2\ g^{-1}$)
VHP/2	1.97		3.995	0.69
α-VP/2	2.00		— [a]	1.05
β-VP/2	1.96		— [a]	2.64
α/β-VP/2	2.02		— [a]	0.85
VP/2–1	n.d. [b]		4.15	n.d. [b]
VP/2–2	2.04		4.20	3.00
VP/2–2′ [c]	n.d. [b]		4.16	2.40
NVP/2	2.01	3.94	— [a]	1.96
$NVP/\frac{3}{4}$	1.01	3.89	4.10	1.62
VP/1	1.00		4.05	n.d. [b]
VP/3	3.00		– [a]	0.48

[a] No valence state determined because of low solubility.
[b] Not determined.
[c] Reproduction of VP/2–2.

rate=10 K/min) in the presence of an ammonia/air/water vapour-containing flow (molar ratio of 1 : 6 : 5.5; 12.5 l/h total flow) [21].

$V(PO_3)_3$ (VP/3) was prepared by heating of V_2O_5 (0.055 mol) and H_3PO_4 (1.72 mol) at 803 K for 3 h (heating rate=10 K/min) under air according to Ref. [23]. $(NH_4)_2(VO)_3(P_2O_7)_2$, containing mixed-valence (V^{IV}/V^{V}) vanadium oxides ($NVP/\frac{3}{4}$), was generated from $VOHPO_4{\cdot}1/2H_2O$ (VHP/1) (0.029 mol) by transformation in an ammonia/air/water vapour flow (molar ratio of 1 : 7 : 5.5; 13 l/h total flow) at 673 K for 5 h [7]. $(VO)_2P_2O_7$ (VP/1) was obtained by calcination of a VHP/1 precursor synthesized in an aqueous medium in accordance with Ref. [24].

All materials were pelletized (20 MPa, ca. 0.5 min) and crushed, thereafter, sieve fractions of 1.25–2.5 mm (oxidation) and 1–1.25 mm (ammoxidation) were applied.

2.2. Characterization of the VPO precursors and catalysts

Fresh and used VPO samples were characterized by chemical analysis (V, P, N, H). The average vanadium valence state was determined by potentiometric titration [11]. The crystallinity as well as a possible phase transformation were investigated by recording X-ray diffraction patterns of the samples with a Stoe automatic transmission powder diffractometer (STADIP), using CuK_{α_1} radiation. The samples were characterized by TG/DTA (heating rate=10 K/min, nitrogen) in order to observe their thermal behaviour (STA/QMS 409C; Netzsch). The surface areas of the fresh and used specimens were determined using the 5-point-BET method (Gemini III; Micromeritics). Furthermore, some samples were characterized by FTIR spectroscopy (KBr technique) in order to observe different V–O, P–O as well as N–H vibrations of ammoxidation catalysts (IFS 66; Bruker). Selected characterization results of the materials are summarized in Table 1.

2.3. Catalytic measurements

The *n*-butane oxidation was carried out in a fixed-bed tubular reactor. The volumes of the different catalyst fillings were in the 2–42 ml range. A feed composition of 1.46 vol% *n*-butane in air was used. The reaction was performed in the 663–773 K range. A *W/F* of 50–150 g h mol^{-1} was applied. *n*-Butane and partially oxidized products were determined by on-line capillary GC (WCOT-FS, 25 m×0.32 mm, FFAP-CB coating; Chrompack) equipped with an FID as detector. For each series of experiments a calibration with defined mixtures of furan/N_2 and MA/N_2, respectively, was carried out.

In the ammoxidation experiments, a fixed-bed U-tube quartz-glass reactor (1.5 ml catalyst volume) was used. The experiments were carried out under the following conditions: toluene : NH_3 : air : H_2O= 1 : 4.5 : 32 : 24, atmospheric pressure, *W/F*= 10 g h mol^{-1}, 673–723 K. Toluene conversion and

yield of aromatic products were followed by on-line capillary GC (FS-SE-54-CB, 25 m×0.25 mm; Chrompack) using an FID as detector.

The total oxidation products CO and CO_2 were determined by non-dispersive infrared photometry (Infralyt 40E, Junkalor). The limit of detection for each compound was 0.01 vol%.

The catalysts were heated under nitrogen to the reaction temperature applied (for *n*-butane oxidation) and to ca. 393 K (ammoxidation runs), respectively. Then the nitrogen flows were replaced by the feeds and 0.5–1 h (oxidation) and 6 h (ammoxidation), respectively, were given for reaching the steady state.

3. Results and discussion

3.1. Characterization of the parent and used samples

As shown in Table 1, the chemical composition of the precursor VHP/2 and the fresh oxovanadium polyphosphate catalysts are in good agreement with the theoretical values. Both the *N*-containing samples show nearly the theoretical values in P/V and H/N molar ratios. The V valence state of NVP/$\frac{3}{4}$ reflects a certain proportion of V^V in the additional mixed-valence vanadium oxide phase formed during the precursor/catalyst transformation [7,25]. As expected, the average vanadium valence state of the VHP/2 precursor amounts to 4.0, whereas the V valence states of 4.15, 4.2 and 4.16, respectively, in case of the amorphous sample VP/2–1 as well as partly crystalline solids VP/2–2 and VP/2–2′ obtained by calcination in air for different times (6 h and 24 h, respectively) and temperatures (673 and 773 K, respectively) exhibit a remarkable oxidation of $V^{IV} \Rightarrow V^V$. Unfortunately, the crystalline specimens α- and β-VP/2 as well as VP/3 are only partly soluble in dilute sulphuric acid and, therefore, a precise determination of valence states of vanadium was impossible in this series of samples.

The BET surface areas of all parent samples are rather low (0.5–3.0 m^2/g).

The XRD patterns of VHP/2, α-VP/2, β-VP/2 and NVP/2 are shown in Fig. 1. The intense reflections of the patterns reveal a high crystallinity of the samples. The XRD study of sample VP/2–1 reveals an amorphous nature of the solid whereas sample VP/2–2 displays a partly crystalline structure as mentioned above.

The TG/DTA curves of VHP/2 show a sharp endothermic transition at ≈678 K with a total weight loss of 13 wt%. A XRD-amorphous material is generated under these conditions. This corresponds to the transformation of VHP/2 to amorphous VP/2 as previously described [20,22,26]. α-VP/2 and β-VP/2 exhibit no thermal signal during DTA. In contrast,

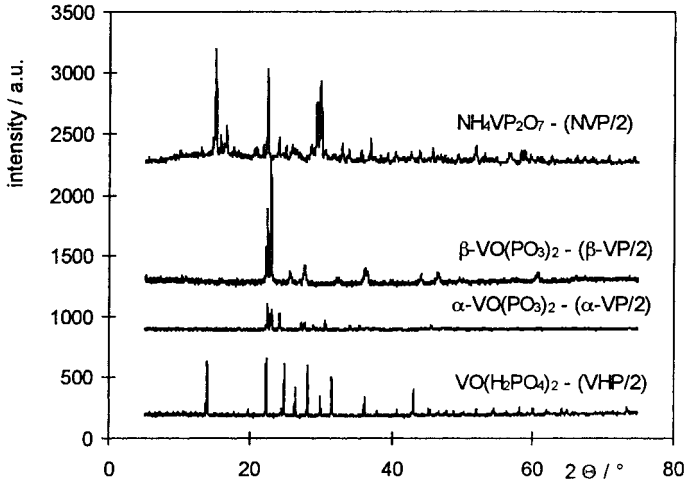

Fig. 1. XRD patterns of the precursor compound $VO(H_2PO_4)_2$ (VHP/2) and the α-$VO(PO_3)_2$ (α-VP/2), β-$VO(PO_3)_2$ (β-VP/2) and $NH_4VP_2O_7$ (NVP/2) catalysts.

NVP/2 shows two endothermic transitions at ≈933 and 1073 K with weight losses of 7.7 wt% and 3.8 wt%, respectively, as calculated if an oligophosphate is assumed to be the final product.

The VHP/2 to β-VP/2 transformation has also been confirmed by means of FTIR spectroscopy. The IR spectrum of the generated NVP/2 demonstrates the presence of ammonium ions (ca. 1420 and 1440 cm^{-1}), the formation of P–O–P links (ca. 950 cm^{-1}) as well as the disappearance of V=O bands (980–1000 cm^{-1} region).

The catalyst samples were also characterized after testing during oxidation and ammoxidation runs. The crystalline samples α- and β-VP/2 remained unchanged after oxidation experiments as revealed by XRD. In contrast, the XRD pattern of the amorphous VP/2-1 after catalytic test shows some reflections of α-VP/2 and some small reflections of β-VP/2 besides a high background, pointing to the existence of large amounts of the original amorphous phase. However, this transformation has also been confirmed by FTIR spectroscopy. After the ammoxidation experiments, no changes in either the composition or crystallinity of α- VP/2, β-VP/2, α/β-VP/2, VP/3 and NVP/2 were observed by XRD. VP/2-1 remained unchanged as amorphous solid. However, chemical analysis revealed that ammonium ions must be present in surface regions of the catalysts but the quantities of defined, crystalline compounds were too small to be detectable by XRD, probably.

The BET surface areas of all catalysts used proved to be as low as those before the tests (0.7–2.4 m^2/g).

3.2. Catalytic results

In Table 2 and Fig. 2 the results of the oxidation of *n*-butane on the catalysts α-VP/2, β-VP/2, VP/2–1 and VP/2–2 are depicted and, for comparison, some data with respect to the catalytic properties of VP/1 and VP/3 in this reaction are also described.

Table 2 shows that the MA selectivities of VP/2-1 and VP/2-2 samples were of the same order of magnitude as those of the crystalline α- and β-VP/2 catalysts and did not exceed 40%. At the same *n*-butane conversion degree, the MA selectivity of the VP/1 sample amounts to more than 70%. On α- and β-VP/2, only traces of furan were found in the reaction products besides very small amounts of other partial oxidation products like acrylic acid and acetic acid. In contrast, on the VP/2-2 samples higher yields of furan (maximum 3%) and acrolein (maximum 6%) were determined. Also, the products of the total oxidation

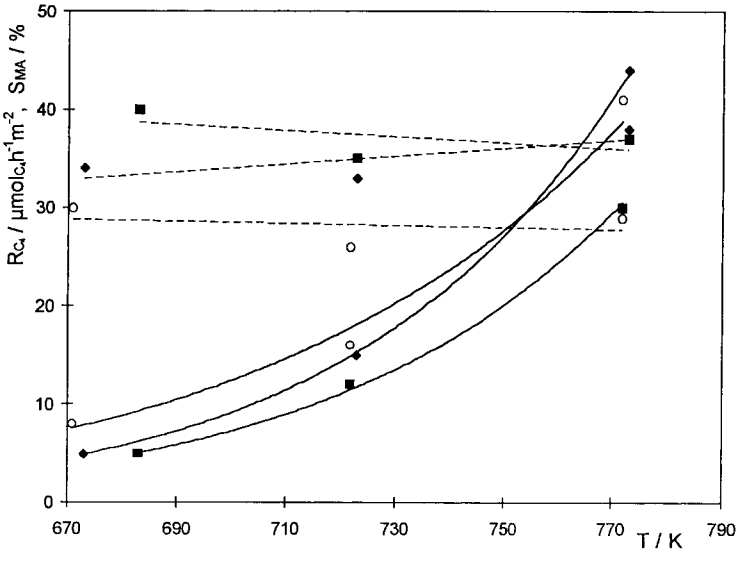

Fig. 2. Specific rate per area of *n*-butane conversion (R_{C_4} /µmol$_{C_4}$ h^{-1} m^{-2}; ———) and maleic anhydride formation selectivity (S_{MA}/%; - - -) on α-$VO(PO_3)_2$ (α-VP/2; ◆), β-$VO(PO_3)_2$ (β-VP/2; ■) and $V(PO_3)_3$ (VP/3; ○) in relation to the reaction temperature (1.46 vol% *n*-butane/air, atmospheric pressure, *W/F*=90–133 g h mol^{-1}, see Table 2).

Table 2
n-Butane conversion (C_{C_4}), selectivity of maleic anhydride (S_{MA}), CO+CO_2 (S_{CO+CO_2}), furan (S_f), acrolein (S_{acr}) and acetic+acrylic acid ($S_{hac+hacr}$) formation as well as specific rate per area of *n*-butane conversion (R_{C_4}) and maleic anhydride formation (R_{MA}) on selected P/V=2 catalysts during oxidation runs (1.46 vol% *n*-butane/air, atmospheric pressure)

Sample	T K	W/F g h mol^{-1}	C_{C_4} %	S_{MA} %	S_{CO+CO_2} %	S_f %	S_{acr} %	$S_{hac+hacr}$ %	R_{C_4} µmol$_{C_4}$ h^{-1} m^{-2}	R_{MA} µmol$_{MA}$ h^{-1} m^{-2}	BET surface area [f] m^2 g^{-1}
α-VP/2	673	90	3.7	34	65	tr [e]	tr [e]	tr [e]	4.5	1.5	1.16
β-VP/2	683	102	7.3	37	67	tr [e]	tr [e]	tr [e]	4.6	1.8	2.01
VP/2–1	773	50	13.5	34	65 [c]	tr [e]	2	3	51.6	19.6	0.66
VP/2–2	671	4	5.7	30	39 [a]	2	5	12	95.5	18.9	2.40
VP/2–2′ [g]	663	6	6.6	n.d. [d]	53 [b]	3	6	16	72.3	14.2	2.40
VP/3	671	133	4.7	30	69	n.d. [d]	n.d. [d]	n.d. [d]	7.7	2.3	0.63
VP/1	673	21	85.6	64	37	0	n.d. [d]	1	34.1	29.2	12.9
VP/1	683	2	9.1	78	25	0	n.d. [d]	n.d. [d]	60.8	47.6	12.9

[a] 0.09 vol% CO, 0.04 vol% CO_2.
[b] 0.15 vol% CO, 0.06 vol% CO_2.
[c] 0.34 vol% CO, 0.11 vol% CO_2.
[d] Not determined.
[e] Traces.
[f] Used samples.
[g] Reproduction of sample VP/2–2.

were found on all catalysts at the lowest *n*-butane conversion. At a conversion degree lower than 5%, the concentrations of both CO and CO_2 were below 0.1 vol%. Only at an *n*-butane conversion of higher than 6%, the concentration of CO exceeded 0.1 vol% and the formation of more than 0.1 vol% CO_2 requires a higher *n*-butane conversion than 13% (see Footnotes a–c of Table 2).

These findings are in contrast to the conclusions drawn by Sananes et al. [20], that at low *n*-butane conversion only the products of selective oxidation, MA and furan, are formed on vanadyl polyphosphate catalysts. The catalysts were obtained from a $VO(H_2PO_4)_2$ precursor which was synthesized using a different method (see [20]) as in this work. However, one of the catalyst specimens applied was prepared by the same calcination procedure as used in case of the samples VP/2–2 and VP/2–2′. Therefore, the difference in selectivities may rather be explained by the higher sensitivities of the analytical methods used in this work in comparison to the GC with packed columns applied in Ref. [20]. For instance, the detection limits of $\leq$0.1 vol% mentioned in Refs. [20,27] for the determination of both CO and CO_2 do not allow determination of the total oxidation products at an *n*-butane conversion of less than 5%. Furthermore, using capillary GC it is possible to separate furan from acetone and acrolein. This separation problem is difficult to solve using packed GC-columns and this may be one of the reasons why comparatively high furan selectivties are described in Ref. [20] which could not be confirmed in any case by our work.

The specific rates per area of MA formation of the several amorphous VP/2 specimens are considerably higher than that of the crystalline polyphosphates. However, they depend remarkably on the duration and the temperature of calcination: Only two samples, VP/2–2 and VP/2–2′, which were calcined at 773 K for 24 h under aerobic conditions show a high specific rate per area of MA formation, comparable to that of the VP/1 sample. In case of sample VP/2–1, which was calcined under milder conditions (673 K, 6 h), a reaction temperature >100 K was necessary to reach a comparable specific rate per area. (The significantly higher conversion degree of *n*-butane of 85.6% at 673 K on VP/1 is due to the remarkably larger BET surface.)

These latter findings are in agreement with the results of Sananes et al. [20] who have found high specific rates per area of MA formation to be typical for amorphous catalysts pretreated for 24 h at 773 K. In case of the VP/2–2 catalysts, this behaviour may be explained by the considerable oxidation of the amorphous solids during the pretreatment in air for 24 h. After this procedure, the catalysts VP/2–2 and VP/2–2′ had average valence states of vanadium of 4.16 and 4.2, pointing to a deep change in the composition of the surface layers and of the subsurface bulk. Possibly, a similar local arrangement of VO_6 octahedra, as in the surface structure of equilibrated $(VO)_2P_2O_7$, has partly been formed in the surface region of $VO(PO_3)_2$, allowing an easier partial oxidation of $V^{IV} \Rightarrow V^{V}$. This new surface structure is believed to show a better catalytic performance than the original surface of $VO(PO_3)_2$ solids which are built up by corner-sharing VO_6 octahedra chains linked by metaphosphate chains. This is in agreement with the previous detection of $(VO)_2P_2O_7$ in a VPO catalyst with a P/V ratio of 1.8 after its treatment with an *n*-butene-in-air feed at the reaction temperature [15]. However, this phase was not observed by XRD in the used VP/2 catalyst samples of this study, possibly due to the lower reduction power of the *n*-butane-in-air feed applied and comparatively short times-on-stream of the respective samples, not allowing a sufficient crystallization for the detection of $(VO)_2P_2O_7$.

A similar behaviour might be the reason for the surprisingly high catalytic performance of the VP/3 catalyst. As shown in Table 2 and Fig. 2, the specific rate per area of *n*-butane conversion and the MA selectivity of this sample are comparable to the results obtained on the α- and β-VP/2 catalysts. Also, in the case of VP/3, a transformation of the surface layers to areas with a lower P/V ratio (and others with higher P/V ratios) seems to be possible under the influence of oxygen and temperature, leading to an increasing oxidizability of the surface region. This results in catalytic properties being comparable to those of $VO(PO_3)_2$ catalysts.

The catalytic properties of VP/3 are in sharp contrast to previous results [17] which revealed that VPO catalysts with P/V>2.5 show no activity and MA selectivity in the *n*-butane oxidation. The reason for this behaviour might be the different method of preparation of the respective $V(PO_3)_3$ applied in Ref.

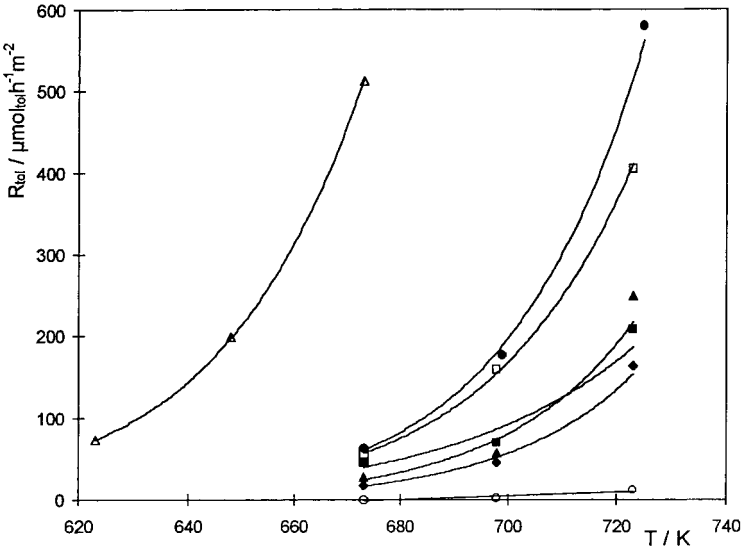

Fig. 3. Specific rate per area of toluene conversion (R_{tol}/µmol$_{tol}$ h^{-1} m^{-2}) on the catalysts used for ammoxidation reaction as a function of the reaction temperature: α-$VO(PO_3)_2$ (α-VP/2, ◆), β-$VO(PO_3)_2$ (β-VP/2, ■), α/β-$VO(PO_3)_2$ (α/β-VP/2, ▲), amorphous $VO(PO_3)_2$ (VP/2-1, □), $NH_4VP_2O_7$ (NVP/2, ●), $V(PO_3)_3$ (VP/3, ○) and $(NH_4)_2(VO)_3(P_2O_7)_2$ (NVP/$\frac{3}{4}$, △) (Toluene : NH_3 : air : H_2O=1 : 4.5 : 32 : 24, atmospheric pressure, W/F=10 g h mol^{-1}).

[17]. In Ref. [17], the calcination was carried out at a very low temperature (523 K for 6 h in air) whereas VP/3 was obtained by calcination in air at 803 K.

All investigated P/V=2 catalysts showed a rather poor catalytic activity (especially for α-VP/2, β-VP/2, α/β-VP/2) in the ammoxidation of toluene as compared to NVP/$\frac{3}{4}$ as shown in Fig. 3 (see also Table 3 for selected results). Similar high specific rates per area for toluene conversion were only reached at reaction temperatures 50–60 K higher than those for NVP/2 and the amorphous VP/2-1. The crystalline polyphosphates (α-VP/2, β-VP/2) exhibited only low toluene conversion (10–20% up to 723 K) under the chosen reaction conditions.

It seems that the structure of these materials, consisting of single vanadyl octahedra chains linked by polyphosphate chains, does not sufficiently permit the series of successive reaction steps of the ammoxidation, i.e. chemisorption of the toluene molecule, H-abstraction, partial oxidation, N-insertion and nitrile desorption [28,29]. To be active enough, catalysts should display close neighboured vanadyl octahedra on the surface as revealed by earlier studies [30,31]. However, it seems that these desired structures are not formed from the parent samples used in this work under the reducing reaction conditions of the ammoxidation.

Thus, VP/1, displaying double chains of two edge-sharing vanadyl octahedra in the crystal volume and other vanadium oxide-containing catalysts (e.g. NVP/$\frac{3}{4}$), the structure of which contains multiples of edge-sharing vanadyl octahedra, exhibits much higher activities (see also Fig. 3). The relatively high catalytic activity observed for NVP/2 (that contains only V^{III} as parent sample) at higher reaction temperatures could be initiated by the same processes as mentioned above for the *n*-butane oxidation, i.e. surface redox processes in the presence of the feed could generate surface areas of the demanded composition and structure units. Unfortunately, due to the low solubility of the resulting catalyst in diluted sulphuric acid the conventional determination of the oxidation state of vanadium failed to prove this assumption of the surface oxidation up to V^{IV}/V^{V}. Furthermore, sufficient amounts of water vapour seem to be necessary that could change the surface properties (e.g. by a hydrolytic break of V–O–P and/or P–O–P links, generation of NH_4^+, initiation of surface redox processes).

In contrast to its activity in the *n*-butane oxidation, VP/3 is not able to convert toluene as only a conver-

Table 3
Toluene conversion (C_{tol}), selectivity of benzonitrile (S_{bn}) and $CO+CO_2$ (S_{CO+CO_2}) formation as well as specific rate per area of toluene conversion (R_{tol}) and benzonitrile formation (R_{bn}) on selected P/V=2 catalysts during ammoxidation runs (Toluene : NH_3 : air : H_2O= 1 : 4.5 : 32 : 24, atmospheric pressure, W/F=10 g h mol^{-1})

Sample	T (K)	C_{tol} (%)	S_{bn} [c] (%)	S_{CO+CO_2} [c] (%)	R_{tol} ($\mu mol_{tol}\ h^{-1}\ m^{-2}$)	R_{bn} ($\mu mol_{bn}\ h^{-1}\ m^{-2}$)	BET surface area [b] ($m^2\ g^{-1}$)
α-VP/2	723	5.4	85	7	164	140	0.56
NVP/2	725	36.2	94	5	581	533	2.15
VP/3	723	0.6	33	tr. [a]	12	4	0.70
NVP/$\frac{3}{4}$	673	48.3	91	8	513	462	1.62

[a] Traces.
[b] Used samples.
[c] Balance: benzaldehyde.

sion of ≈0.5% at 723 K was observed. Obviously, in this case a sufficient oxidation of V^{III} surface regions to V^{IV}/V^{V} areas is hindered, probably by the minor oxidation potential of the ammoxidation feed. Moreover, an enrichment in phosphorus of the surface layer of VPO catalysts should also be considered to have arisen by the content of water vapour in the feed (see Ref. [13]).

Benzonitrile is the main product of the reaction, as expected. The nitrile selectivities amounted to ≈85–95% at higher conversion rates. Surprisingly, minor amounts of benzaldehyde (up to 1%) were found during the catalytic runs, reflecting the inability of these catalysts to activate ammonia to a sufficient extent at lower reaction temperatures. This finding is a further proof of the role of benzaldehyde as a reaction intermediate, as recently shown by in-situ FTIR spectroscopy [29] as well as by temporal-analysis-of-products (TAP) investigation of the ammoxidation reaction on VP/1 [28]. Besides minor amounts of carbon oxides, no other partially oxidized products were found.

4. Conclusions

Amorphous as well as partly crystalline $VO(PO_3)_2$ catalysts show a specific rate per area of MA formation in the *n*-butane oxidation which is comparable to that of $(VO)_2P_2O_7$ catalysts. The reason is probably a structural transformation of the surface region under the influence of excess oxygen. Crystalline $VO(PO_3)_2$ catalysts do not show a comparable surface transformation. Furthermore, it is assumed that the resulting surface structures of the polyphosphate catalysts inhibit the rate of reoxidation, leading to a higher concentration of electrophilic oxygen species which results in increasing total oxidation. Consequently, the MA selectivity on crystalline as well as amorphous $VO(PO_3)_2$ is lower than on $(VO)_2P_2O_7$ catalysts. This effect also occurs at low *n*-butane conversion: Other statements are possibly due to misinterpretation of analytical data.

In contrast to previous statements [17], $V(PO_3)_3$ seems to be attacked by oxygen at comparatively low temperatures, leading to a surface structure which exhibits a specific rate per area of *n*-butane conversion and an MA selectivity comparable to that of crystalline $VO(PO_3)_2$ catalysts. Probably, under the more reducing atmospheric conditions of the ammoxidation feed, these structures cannot be formed. Therefore, $V(PO_3)_3$ shows only little activity in the ammoxidation of toluene.

In ammoxidation, the crystalline oxovanadium polyphosphates reveal a rather poor catalytic activity due to structural reasons, as already discussed. Otherwise, the amorphous polyphosphate and the NH_4^+-containing VPO show relatively high toluene conversion rates caused by easier proceeding surface redox reactions as a consequence of structural transformation of surface areas. These processes should also include the incorporation of NH_4^+. Benzonitrile selectivities up to 95% are reached. Minor amounts of formed benzaldehyde mirror a suppressed ability of these solids to activate ammonia to a sufficient extent at least at lower reaction temperatures.

The studies described above show an interesting dynamics of the structure of the surface region of VPO catalysts with P/V ratios ≥2 during oxidation and ammoxidation experiments. Further investigation of

these phenomena should lead to a better understanding of the activity and selectivity of these materials. Nevertheless, $(VO)_2P_2O_7$ will continue to be the commercially more important *n*-butane oxidation catalyst in future as well.

Acknowledgements

The authors thank Mrs. H. French and Mrs. B. Lange for experimental assistance and the Commission of the European Community for financial support for this work under the Human Capital and Mobility programme (contract ERBCHRXCT930290).

References

[1] Vanadyl pyrophosphate catalysts, G. Centi (Ed.), Catal. Today 16(1) (1993).
[2] E. Bordes, Catal. Today 1 (1987) 499.
[3] F. Cavani, F. Trifirò, Catalysis 11 (1994) 246.
[4] A. Martin, B. Lücke, H. Seeboth, G. Ladwig, E. Fischer, React. Kinet. Catal. Lett. 38(1) (1989) 33.
[5] A. Martin, B. Lücke, H. Seeboth, G. Ladwig, Appl. Catal. 49 (1989) 205.
[6] B. Lücke, A. Martin, in M.G. Scaros, M.L. Prunier (Eds.), Catalysis of Organic Reactions, Marcel Dekker, Inc., New York, 1995, p. 479.
[7] Y. Zhang, A. Martin, G.-U. Wolf, S. Rabe, H. Worzala, B. Lücke, M. Meisel, K. Witke, Chem. Mater. 8 (1996) 1135.
[8] A. Martin, H. Berndt, B. Lücke, M. Meisel, Top. Catal. 3 (1996) 377.
[9] B.K. Hodnett, Catal. Rev.-Sci. Eng. 27 (1985) 373.
[10] L.M. Cornaglia, E.A. Lombardo, Appl. Catal. A: General 127 (1995) 125.
[11] B. Kubias, M. Meisel, G.-U. Wolf, U. Rodemerck, Stud. Surf. Sci. Catal. 82 (1994) 195.
[12] M.R. Thompson, J.R. Ebner, Stud. Surf. Sci. Catal. 72 (1992) 353.
[13] B. Kubias, F. Richter, H. Papp, A. Krepel, A. Kretschmer, Stud. Surf. Sci. Catal. 110 (1997) 461.
[14] H. Morishige, J. Tamaki, N. Miura, N. Yamazoe, Chem. Lett., (1990) 1513.
[15] E. Bordes, P. Courtine, J. Catal. 57 (1979) 236.
[16] U.S. Patent 4,209,423 (1980).
[17] V.A. Zazhigalov, A.J. Pyatnitskaya, G.A. Komashko, V.M. Belousov, Kinet. i Katal. 26 (1985) 885.
[18] G.-U. Wolf, B. Kubias, H. Worzala, M. Meisel, Chem.-Ing.-Tech. 66 (1994) 951.
[19] M.T. Sananes, I.J. Ellison, S. Sajip, A. Burrows, C.J. Kiely, J.C. Volta, G.J. Hutchings, J. Chem. Soc. Faraday Trans. 92(1) (1996) 137.
[20] M.T. Sananes, G.J. Hutchings, J.C. Volta, J. Catal. 154 (1995) 253.
[21] A. Martin, S. Rabe, U. Steinike, B. Lücke, F.K. Hannour, J. Chem. Soc., Faraday Trans. 93(21) (1997) 3855.
[22] G. Ladwig, Z. Chem. 8(8) (1968) 307.
[23] B.C. Tofield, G.R. Crane, G.A. Pasteur, R.C. Sherwood, J. Chem. Soc. Dalton Trans. 18 (1975) 1806.
[24] T. Götze, D. Groke, B. Kubias, M. Meisel, H. Wolf, DE-OS 1 96 450667 (1996).
[25] H. Berndt, K. Büker, A. Martin, A. Brückner, B. Lücke, J. Chem. Soc., Faraday Trans. 91 (1995) 725.
[26] F. Garbassi, J.C.J. Bart, F. Montino, G. Petrini, Appl. Catal. 16 (1985) 271.
[27] M.T. Sananes, private communication.
[28] A. Martin, H. Berndt, B. Lücke, M. Meisel, Top. Catal. 3 (1996) 377.
[29] Y. Zhang, A. Martin, H. Berndt, B. Lücke, M. Meisel, J. Molec. Catal. A: Chemical 118 (1997) 205.
[30] H. Berndt, Y. Zhang, A. Martin, K. Büker, S. Rabe, M. Meisel, Catal. Today 32 (1996) 285.
[31] A. Martin, A. Brückner, Y. Zhang, B. Lücke, Stud. Surf. Sci. Catal. 108 (1997) 377.